

Short communication

The computation of foliage clumping index using hemispherical photography

Alemu Gonsamo*, Petri Pellikka

Department of Geography, University of Helsinki, P.O. Box 64, FIN-00014 Helsinki, Finland

ARTICLE INFO

Article history:

Received 6 March 2009

Received in revised form 31 May 2009

Accepted 3 June 2009

Keywords:

Forest

Hemispherical photography

Leaf area index

Clumping index

ABSTRACT

Hemispherical photography (HP) is extensively used for both canopy architecture such as leaf area index (LAI), and solar radiation regime determinations under forest canopies. This is done mainly by assuming that foliage elements occur in a spatially random manner. However, the majority of world forests occur in heterogeneous ecosystems and topography with rather complex canopy architecture. To improve the estimates of canopy structures and solar radiation regimes, a non-random spatial distribution parameter called clumping index (CI) has been used. We compared varying methodologies of CI determination on real HP acquired in contrasting forest types growing on sloping ground, and on simulated HP representing different aggregation levels of foliage elements. The major aim was the comparative analysis of the effects of forest types, forest density, slope and gap fraction acquisition accuracy on estimation of CI using the five different approaches. The result indicated that CI estimates based on gap size distribution approaches performed the best and were less affected by topography and forest density compared to approaches based on solely logarithmic gap averaging techniques.

© 2009 Elsevier B.V. All rights reserved.

1. Introduction

Hemispherical photography (HP) provides a convenient mechanism to assess forest canopy structure and solar radiation regimes. This technique is well described in literatures and the most widely used ground-based remote sensing method to indirectly quantify leaf area index (LAI), canopy gap fractions and size distributions, leaf angle distributions and specific canopy components such as sunlit and shaded leaves (Jonckheere et al., 2004). Existing HP techniques are mostly based on the use of a simple, or modified, Poisson model to invert gap fraction data (Walter et al., 2003).

In contrast to major Poisson model assumption used in HP analysis for canopy structure and solar radiation determinations, the majority of world forest occurs in heterogeneous ecosystem and complex topography. To improve the estimates of canopy structures and radiation regimes, the non-random spatial distribution parameter called clumping index (CI) has seldom been used. CI determination in forest canopy has usually been overlooked and remains one of the most important challenges in the field of LAI estimation using optical ground instruments. Non-random distribution of foliage elements, i.e., needles, leaves, shoots, branches and crowns in forest canopies leads to underestimation of LAI using a simple random model. The CI quantifies the degree of the deviation of foliage spatial distribution from the random case. The importance

of CI for carbon cycle modeling has also been demonstrated by Chen et al. (2003), as CI allows a better segmentation of the solar radiation distribution in sunlit and shaded leaves as compared to models that relate carbon absorption to the intercepted solar radiation only. Sunlit and shaded leaf stratification is one of the most effective ways to upscale from leaf to canopy in modelling vegetation photosynthesis particularly in boreal forests because of the relatively large shaded leaf fraction in clumped canopies.

Optical field instruments particularly HP provides indispensable advantages on simultaneous acquisition of gap fraction in multiple directions, permanent recordings and spatial discrimination leading to the calculation of foliage clumping. The precision with which the canopy element and gap distributions were quantified allows determining CI which subsequently used to improve indirect measures of LAI and modify Poisson model, making it more applicable for use in discontinuous plant canopies.

Different techniques have been developed to quantify CI based on varying gap fraction averaging methods and gap size distribution theories (Walter et al., 2003; Jonckheere et al., 2004; Leblanc et al., 2005). However, to this day there is no comprehensive comparison of the approaches and the effect of foliage density and topography on CI determination. To this effect, we base our study on the real HP taken on series of contrasting forest types, including natural tropical cloud forest with dense overstorey, dense understorey and sparse overstorey, and *Pinus*, *Cupressus*, and *Eucalyptus* spp. plantations, growing on sloping ground. The performance of varying approaches for CI determination was tested using artificial photographs simulating ideal canopies with varying LAI and aggregation levels of foliage elements.

* Corresponding author. Tel.: +358 9 19150770; fax: +358 9 19150760.

E-mail address: alemu.gonsamo@helsinki.fi (A. Gonsamo).

2. Calculations and algorithms

For both simulated and real HP, the image analysis was restricted to the multiple directions of view zenith angle ranges of 30–60°, as also used by other studies (Leblanc and Chen, 2001; Leblanc et al., 2005). CI can vary with view zenith angle, however, simulations done with Five-scale model have shown that the variation is often very small over the 20–70° range and that the mean CI between 30 and 60° is very close to the mean CI of all angles (Leblanc and Chen, 2001). 30–60° is also useful view zenith angle range for calculation of LAI as the LAI requires the assumption of foliage orientation which can be avoided either by integrating the whole view zenith angle ranges 0 to $\pi/2$ or using only 57° where foliage projections coefficient is nearly always 0.5. In this regard, 30–60° is equally truncated from both zenith and horizon side which results the approximate estimate of the whole field of view. The angle ranges close to zenith result in short segments which may produce erroneous estimates of gap fraction and size distributions. In other hands, those near to horizon have high proportion of mixed pixels due to the light scattering and coarse image resolution. Five approaches have been used to measure the CI using only the 30–60° view zenith angle ranges.

2.1. CI from logarithmic gap averaging method (CI_{LX})

CI_{LX} is computed using a logarithmic gap averaging technique (Lang and Xiang, 1986) as follows:

$$CI_{LX} = \frac{\ln(\overline{P(\theta, \varphi)})}{\ln(P(\theta, \varphi))} \quad (1)$$

where $\overline{P(\theta, \varphi)}$ is the canopy mean gap fraction averaged from sky segments defined by zenith angle θ and azimuth angle φ , and $\ln(P(\theta, \varphi))$ the logarithmic mean gap fractions of all segments. This approach assumes that vegetation elements are locally randomly distributed, i.e., Poisson law is valid at the size of selected segment. The assumption of random foliage may not be true if the logarithm average is calculated for length longer than 10 times the foliage element, since large gaps between crowns give erroneous results, or over very short segments since the Poisson theory used to derive Eq. (2) assumes an infinite canopy to achieve the exponential relationship (Lang and Xiang, 1986). As the logarithm of zero is undefined, for 'empty segments', to allow the calculation of the logarithm of gap fraction, a new value of gap > 0 is computed, using a local Poisson model, Walter (2008) and Leblanc et al. (2005):

$$P(\theta, \varphi) = \exp\left(\frac{-0.5LAI_{sat}}{\cos\theta}\right) \quad (2)$$

where LAI_{sat} is maximum (saturated) LAI:

$$LAI_{sat} = -2 \ln\left(\frac{1}{N_{pixels}}\right) \cos\theta \quad (3)$$

where N_{pixels} is the number of pixels in an empty segment. For example, if $LAI_{sat} > 8$ (an arbitrary fixed upper limit to LAI), LAI_{sat} is forced to 8. Based on the in house analysis (Gonsamo et al., submitted for publication), we selected the equiangular segments size of 5°, both in zenith and azimuth directions.

2.2. CI from modified logarithmic gap averaging method (CI_W)

CI_W is based on a hierarchical logarithmic averaging of gap fractions over azimuth (Walter et al., 2003; Walter, 2008). Gap fractions are first linearly averaged over azimuths of variable angular widths. Logarithms of these averages are taken to give 'logarithmic means'. For each zenith angle considered, azimuthal

resolution (Φ) varies in a hierarchical manner:

$$\overline{\ln(P_0)} = \frac{1}{x-y+1} \sum_{j=1}^{x-y+1} \ln\left[\frac{1}{y} \sum_{i=j}^{j+y-1} P_{ij}\right] \quad (4)$$

where $\overline{P_0}$ is the gap fraction linearly averaged over specified azimuthal resolution, assuming randomness at this scale, y is the determined set of azimuthal sectors out of the total number of x sectors (72 based on 5° sector width), i and j are counters based on θ , φ and Φ . y varies according to the determined azimuthal resolution Φ , in this case 5° of sector width. For example, if Φ is 90°, $y = \Phi/5^\circ = 18$. Finally the clumping index is computed as:

$$CI_W = \frac{P(\theta, \varphi)}{\ln(\overline{P_0})} \quad (5)$$

Thus, in this study, CI_W is computed as a ratio of full arithmetic average of gap fractions ($P(\theta, \varphi)$), i.e., $y = 72$ resulting in 360° of Φ , and of full geometrical average of gap fractions ($\ln(\overline{P_0})$), i.e., $y = 1$ resulting in 5° of Φ in Eq. (4). It is possible to compute CI using several other spatial scales in a hierarchical manner, at scales where no empty segments are detected.

2.3. CI from gap size distribution (CI_{CC})

CI_{CC} is computed based on the gap size and fraction analysis (Leblanc, 2002; Leblanc et al., 2005):

$$CI_{CC} = \frac{\ln[F_m(0, \theta)] [1 - F_{mr}(0, \theta)]}{\ln[F_{mr}(0, \theta)] [1 - F_m(0, \theta)]} \quad (6)$$

where $F_m(0, \theta)$ is the measured accumulated gap fraction larger than zero, i.e., the canopy gap fraction, and $F_{mr}(0, \theta)$ is the gap fraction for the canopy when large gaps that are not theoretically possible in a random canopy have been removed for a given LAI and foliage element width. CI_{CC} takes the advantages of both the gap fraction and the gap size information, which can be applied to all types of plant canopies without the need for spatial pattern assumptions about canopy elements unlike logarithmic gap fraction averaging methods.

2.4. CI from combination of gap size and logarithmic averaging method (CI_{CLX})

CI_{CLX} is calculated based on the combination of concepts used in CI_{LX} and CI_{CC} to address both segment size related problem in logarithmic gap averaging method when large gaps are not homogeneous and the within segment heterogeneity using gap size distribution theory (Leblanc et al., 2005):

$$CI_{CLX} = \frac{n \ln[\overline{p(\theta, \varphi)}]}{\sum_{k=1}^n \ln[P_k(\theta, \varphi)] / CI_{CCK}(\theta, \varphi)} \quad (7)$$

where $CI_{CCK}(\theta, \varphi)$ is the element clumping index of segment k using the CI_{CC} method and $P_k(\theta, \varphi)$ is the gap fraction of segment k . The CI_{CLX} is computed over n number of segments and integrated over the zenith angle ranges considered.

2.5. CI from Pielou's coefficient of spatial segregation (CI_{PCS})

CI_{PCS} is originally a coefficient of segregation of one species to another in plant population, as suggested by Pielou (1962). It was later applied to hemispherical photography by Walter et al. (2003) and Walter (2008). Using the zenithal transects of sequences of B (background representing foliage) and W (foreground representing gap) pixels from gap size distribution, the probability of encountering pixel B and W are b and w , respectively, and for

randomly distributed pixels $b + w = 1$. Therefore, CI_{PCS} is calculated assuming that if the B and W are dispersed at random, it follows that with 95% probability:

$$CI_{PCS} = \hat{b} + \hat{w} = \frac{1}{\hat{m}_B} + \frac{1}{\hat{m}_W} = 1 \pm 1.96 \sqrt{S_B^2 + S_W^2} \quad (8)$$

where \hat{b} and \hat{w} are the maximum likelihood estimates of B and W pixels, \hat{m}_B and \hat{m}_W are the mean lengths of B and W in numbers of pixels; S_B^2 and S_W^2 are the variances of B and W pixels with regard to \hat{b} and \hat{w} , respectively. Variances are calculated as:

$$S_B^2 = \frac{1}{n_W} \frac{\hat{m}_W - 1}{\hat{m}_W^3} \quad \text{and} \quad S_W^2 = \frac{1}{n_B} \frac{\hat{m}_B - 1}{\hat{m}_B^3} \quad (9)$$

where n_B and n_W are the numbers of sequences of B and W pixels, respectively. Thus, Pielou's coefficient of segregation is defined as a single value of $\hat{b} + \hat{w}$ from HP analysis and assumed to be equivalent of foliage element clumping index: CI_{PCS} .

All the five approaches used to compute CI are calculated either from gap fraction and/or gap size distribution data derived solely from HP without the knowledge of the foliage orientation or destructive sampling. Hence, in all cases, CI is interpreted in the same manner, i.e., $CI = 1$, foliage elements are randomly distributed; $CI > 1$, foliage elements are regularly distributed (rare case, foliage elements are laid side by side); and $CI < 1$, foliage elements are clumped (common case, foliage elements are stacked on top of each other).

3. Tests

3.1. Software

The clumping index algorithms were implemented into a software package of programs designed to analyse hemispherical photographs for canopy geometry and solar radiation assessment (Walter, 2008). This software, called CIMES, is available as freeware from the following web site: <http://equinox.u-strasbg.fr/cimes>. The simulated canopy photographs were generated within a 3D matrix to formulate a horizontally extended foliage distribution by applying a ray tracing algorithm using the program called ULoopPS (for Upward Looking Photography Simulator; Fournier et al., 1996; Walter et al., 2003).

3.2. Simulated photographs

The photographs simulated for the work of Walter et al. (2003) were used. The photographs were simulated within a 3D forest stand for a range of simulated, true LAI values 2, 3 and 6, and clustering percentage (fractional clumping, Fc) ranging from 0 to 1 by increments of 0.1 providing a total of 33 combinations. For details and procedures on simulating 3D spatial distribution of foliage, i.e., foliage clumping, we refer to the work of Walter et al. (2003) and Fournier et al. (1996). Calculations were applied to a rectangular volume with 5 m per horizontal side and 10 m of height and composed of small opaque cells with dimensions of 10 cm per horizontal side and 1 cm of height. Cells simulated a horizontal flat leaf with a thickness of 1 cm. The number of opaque cells was calculated from the total LAI selected while taking into account an LAI contribution of each 0.01 m² cell. Fc is a percentage applied to the Euclidean distance separating a leaf from its closest clump centre. Fc = 0 corresponds to a random foliage distribution, and when Fc = 1 all the leaves are compacted into a point corresponding to their associated cluster seed. The forest stand was simulated by placing side to side, with no space, a copy of the same 3D volume until sufficient horizontal extent was reached. The bases of the volumes were placed at a height of 10 m to

simulate a vertical distribution of foliage between 10 and 20 m. A 600 m × 600 m forest stand was simulated to reduce the border effects at large view angles on the HP. HP were simulated at the centre of the stand at 1.5 m above the ground to recreate a possible scenario. The ray tracing simulations resulted in an image formed only by black (0, obstructed ray) and white (1) pixels with a resolution of 1024 × 1024 pixels.

3.3. Real photographs

Real photographs were acquired in the forest fragments of Taita Hills, South-East Kenya (03°15' to 3°30'S, and 38°15' to 38°30'E). The experimental setup was first designed to study the slope effect on LAI estimation using HP. The details of the study site description can be found in Gonsamo and Pellikka (2008). A total amount of 81 HP pairs were taken in a series of contrasting forest types, including natural tropical cloud forest with dense overstorey ($n = 26$), dense understorey ($n = 19$) and sparse overstorey ($n = 7$), and *Pinus* ($n = 9$), *Cupressus* ($n = 12$), and *Eucalyptus* spp. ($n = 8$) plantations, growing on sloping ground (5–29°) were tested as real canopies. The photographs were acquired using 8 mega pixels Nikon Coolpix 8800 VR digital camera equipped with a fish-eye Nikon FC-E9 lens adapter. Photographic acquisition procedures, including orientation for slope measurements are described in Gonsamo and Pellikka (2008), except that only photographs acquired on slope < 30° were used in this study to avoid the interference of topography on CI calculations. Two types of HP were taken from each sampling point: (1) normal to a horizontal surface (optical axis oriented to local zenith), hereafter referred to as 'levelled' and (2) normal to the slope of the ground (fish-eye lens oriented parallel to slope), hereafter referred to as 'tilted'. To separate sky from foliage, a single threshold was set visually. All photographs were pre-processed prior to the image analysis software. The pre-processing included orienting the photographs, centring (identifying the circular limit or horizon of the photograph), selection of appropriate colour channel (in this case blue channel, in order to improve the contrast between vegetation and sky), defining the threshold and storing in 8 bit grey scale format with 0 (foliage) and 255 (gap) binary values.

4. Results and discussion

4.1. Simulated photographs

When the whole fractional clumping (Fc) and simulated LAI range is considered, CI_{CLX} gave CI values close to expected values (Fig. 1). However, CI_{CLX} is not very sensitive for lower and higher foliage clumping and apart from high foliage clumping (low CI), CI_{CLX} values are similar with CI_{CC} estimates. Besides, CI_{CLX} estimates are consistent with the three simulated LAI values. Except that for lower and higher foliage clumping (Fc: 0.1–0.6), the result obtained using CI_{PCS} is the closest to expected value than all other approaches (Fig. 1). This CI range (Fc: 0.1–0.6) is realistic range which perhaps can be occurred in real canopies. As shown in Leblanc et al. (2005) where CI_{LX} , CI_{CC} and CI_{CLX} are consistent in variation along zenith angles of only 30–60°, these three estimates in this study shown also consistent variation only for narrow range of simulated Fc. Both logarithmic approaches, i.e., CI_{LX} and CI_W generally gave unrealistic results in most of the cases (Fig. 1). Considering the overall performances of all five methods applied to estimate CI, CI_{CLX} performed best in most cases both in consistency of estimates along the simulated LAI and Fc ranges. None of the five methods employed here showed linear response of CI to changing Fc and LAI. Our result is in good agreement with that of Walter et al. (2003) where they demonstrated detailed analysis of CI_{CC} and CI_{PCS} . Note that except that of CI_{PCS} for lower simulated LAI values,

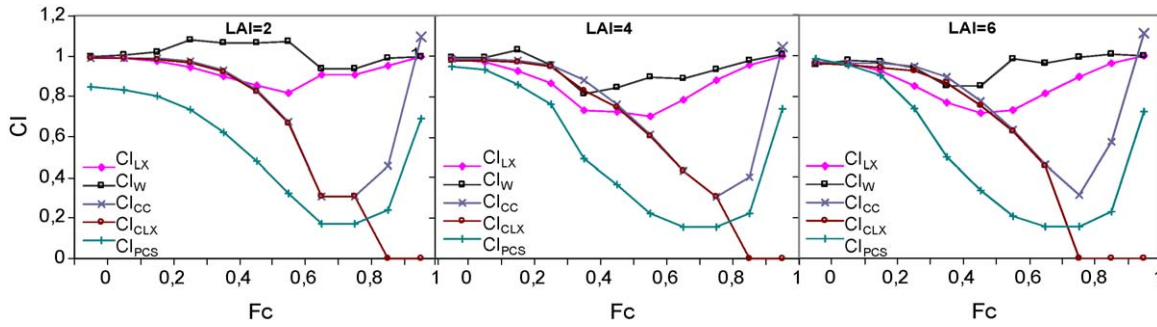


Fig. 1. Clumping index estimated using five methods from simulated photographs having a theoretical LAI of 2, 4 and 6.

all the methods gave realistic results for random or near to random foliage element simulations (Fig. 1).

The LAI (calculated using Miller's integral theorem, Miller, 1967) corrected for non-random distribution of foliage elements using CI computed using the five approaches only for realistic Fc ranges (0.1–0.6) is presented in Fig. 2. Considering the overall performance, LAI corrected with Cl_{CC} is performed best with 18% average deviation from real values followed by Cl_{CLX} deviating by 19% from real values and the least being Cl_{PCS} by deviating 52% above the real values. For lower simulated LAI value of 2 and 4, Cl_W close to real average values to (Fig. 2) but with higher standard deviation. Considering both the average and the standard deviation of the estimates, both Cl_{CC} and Cl_{CLX} performed best compared to other approaches and in good agreement with other studies (Walter et al., 2003; Leblanc et al., 2005).

4.2. Real photographs

The CI estimates from both levelled and tilted acquisitions do not show major sensitivity for varying forest types studied in all five approaches (Fig. 3). CI is generally not very sensitive parameter for varying species or forest canopy types (e.g., Leblanc et al., 2005). Conifers are known to have higher overall clumping (low clumping index) compared to broadleaved species due to needle clumping on shoots. However, HP does not detect all small gaps between needles therefore most of the CI computed for *Pinus* and *Cupressus* spp. are the values comprised for shoot level and larger structures. Besides, the larger footprint (360° in azimuth) of the HP probably tends to average the conditions to a value that may be more representative of a larger area resulting into similar CI for varying forest types. It must be noted, however, that neither the needle leaved nor broadleaved CI from HP are necessary wrong, they just represent different levels of clumping in forest canopies. Clumping

of canopy elements occurs in a hierarchical way in all forests: rosettes of leaves, shoots, crownlets, crowns, trees, tree clusters, forest patches (Fournier et al., 1997). In broad leaved canopies, the unit photosynthetic canopy element is the leaf whereas, in conifer canopies, the basic foliage unit is the shoot. Broad leaves are no less clumped than conifer needles, an observation that is generally overlooked (Walter, 2008). This explains by the fact that HP cannot detect the amount of needle area in a shoot, when the shoot is too dense to allow light penetration for deriving gap fractions.

The real HP CI ranges are smaller compared to simulated HP. Unlike the most cases of the simulated HP CI estimates, both Cl_{CC} and Cl_{CLX} resulted in higher CI (lower foliage clumping) in all cases except that of tilted acquisition on sparse overstorey forest fragment. Except that of Cl_W, all the four estimates are consistent in deference obtained among the forest types and acquisition methods. Cl_{LX} and Cl_{PCS} consistently gave lower CI estimate in all forest types and in both acquisition methods (Fig. 3). This is in good agreement with the simulated HP result for moderately clumped Fc range between 0.0 and 0.5 (Fig. 1). All the CI were significantly correlated ($P < 0.01$) per acquisition methods except that Cl_W did not show any correlation in the cases of tilted acquisition. The highest correlations were obtained among Cl_{CC}, Cl_{CLX} and Cl_{PCS} ($R^2 > 0.7$).

Slope has substantial effect on CI calculations (Tables 1 and 2, Fig. 4). The overall mean of CI index is higher in tilted acquisition method in all five CI calculation approaches (Table 1). Except that of Cl_{CC} and Cl_{CLX}, the mean CI estimates from the remaining approaches resulted in statistically different average (Table 1, $P = 0.05$). The main differences are obtained for logarithmic gap averaging methods (Cl_{LX} and Cl_W, Fig. 4). In contrary to this study, Macfarlane et al. (2007) suggested the use of the Cl_{LX} method for correcting foliage clumping in preference to Cl_{CC} method, unless the gap size distribution is known to be very accurate. The main reason for higher foliage clumping in the cases of levelled acquisition is that the levelled HP in sever slope areas result in bigger gaps in downslope sky segments compared to upslope which in turn gives erroneous CI particularly in the cases of logarithmic and azimuthal gap averaging methods which rely on the whole canopy gap fractions (Gonsamo and Pellikka, 2008). On the other hand, CI based on the gap size distribution theories are less affected by slope due to the fact that they are sensitive mainly for smaller gap sizes.

Although both logarithmic methods gave statistically different mean ($P > 0.05$), the difference obtained in Cl_W is more erratic (Table 2, Fig. 4) compared to Cl_{LX} which is more systematic and gave statistically significant correlation (Table 2, $P < 0.01$). 30% of CI which were underestimated using levelled acquisition compared to tilted acquisition using Cl_W where overestimated using Cl_{LX}. Only 70% have the same direction of change of CI compared for acquisition types for these two methods despite the fact that both are based on logarithmic gap averaging approaches. Whereas, 91%

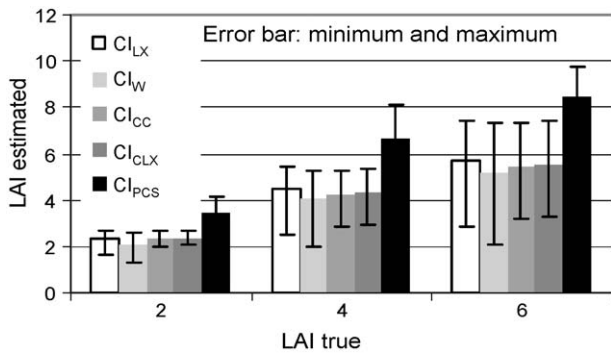


Fig. 2. Mean LAI estimated using Miller's integral theorem (Miller, 1967) corrected for foliage clumping using five methods from simulated photographs having a theoretical LAI of 2, 4 and 6. Both CI and LAI values are calculated only for Fc range between 0.1 and 0.6.

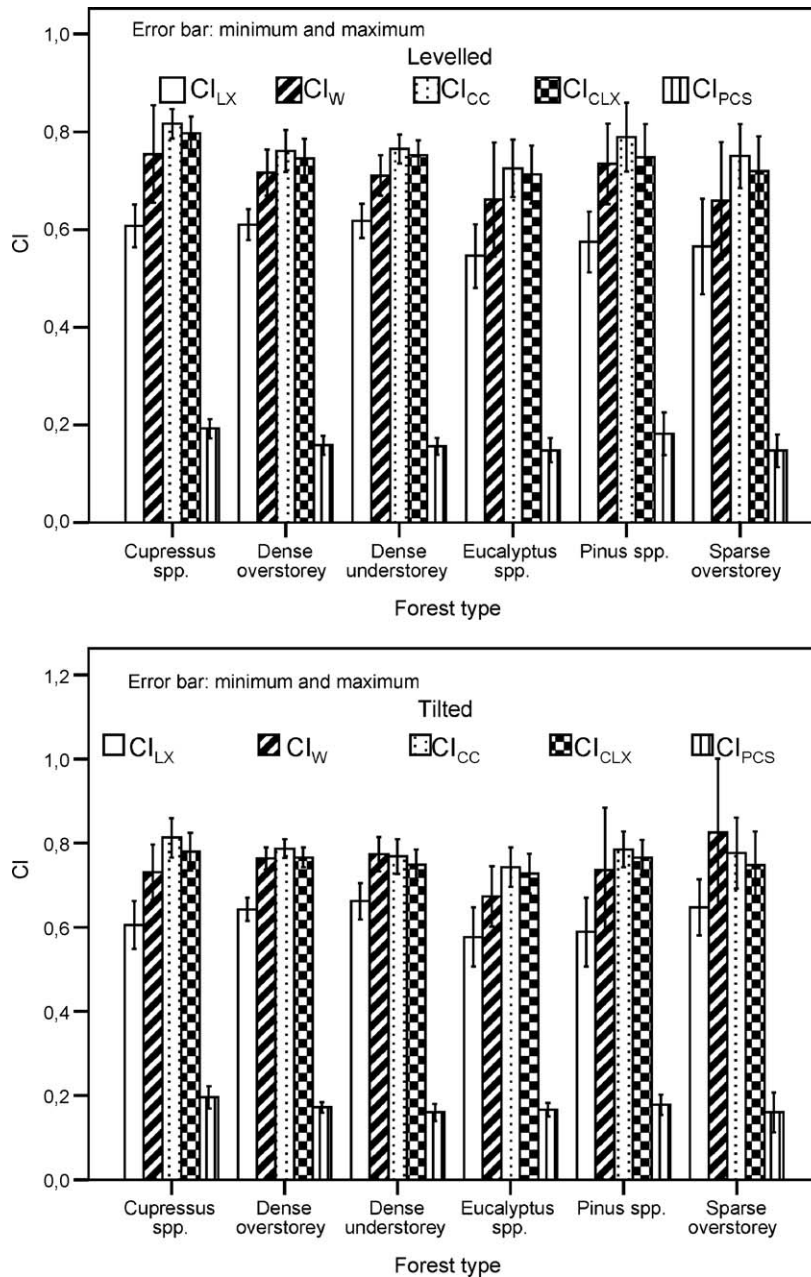


Fig. 3. Clumping index estimated using five methods for real photographs acquired from levelled and tilted acquisition methods plotted against forest types.

of $CI_{CC}-CI_{PCS}$, 90% of $CI_{CC}-CI_{CLX}$, 64% of $CI_{LX}-CI_{CLX}$, and 67% of $CI_{LX}-CI_{CC}$ resulted in the same direction of change of estimated CI compared for acquisition types. Fig. 4 shows the clear resemblance of CI_{CC} and CI_{PCS} per acquisition type. The only difference between CI_{CC} and CI_{PCS} is that the first is based on a gap size accumulation

Table 1
Mean ($n = 81$) clumping index averaged over all-embraced forest types from levelled and tilted acquisitions.

Clumping index	Levelled	Tilted	Sig. (2-tailed)
CI_{LX}	0.597	0.629	0.000
CI_W	0.712	0.754	0.003
CI_{CC}	0.769	0.781	0.095
CI_{CLX}	0.750	0.758	0.173
CI_{PCS}	0.163	0.172	0.019

Table 2
Pearson correlation coefficient of clumping index estimated using five methods for real photographs from levelled and tilted acquisitions.

Tilted	Levelled				
	CI_{LX}	CI_W	CI_{CC}	CI_{CLX}	CI_{PCS}
CI_{LX}	0.50**	0.12	0.12	0.20	0.11
CI_W	0.09	-0.05	0.14	0.08	0.14
CI_{CC}	0.34**	0.20	0.41**	0.43**	0.40**
CI_{CLX}	0.43**	0.27*	0.41**	0.46**	0.40**
CI_{PCS}	0.23*	0.19	0.38**	0.41**	0.49**

In bold, Pearson correlation coefficient values for the same methods from levelled and tilted acquisitions.

** $P < 0.01$.

* $P < 0.05$.

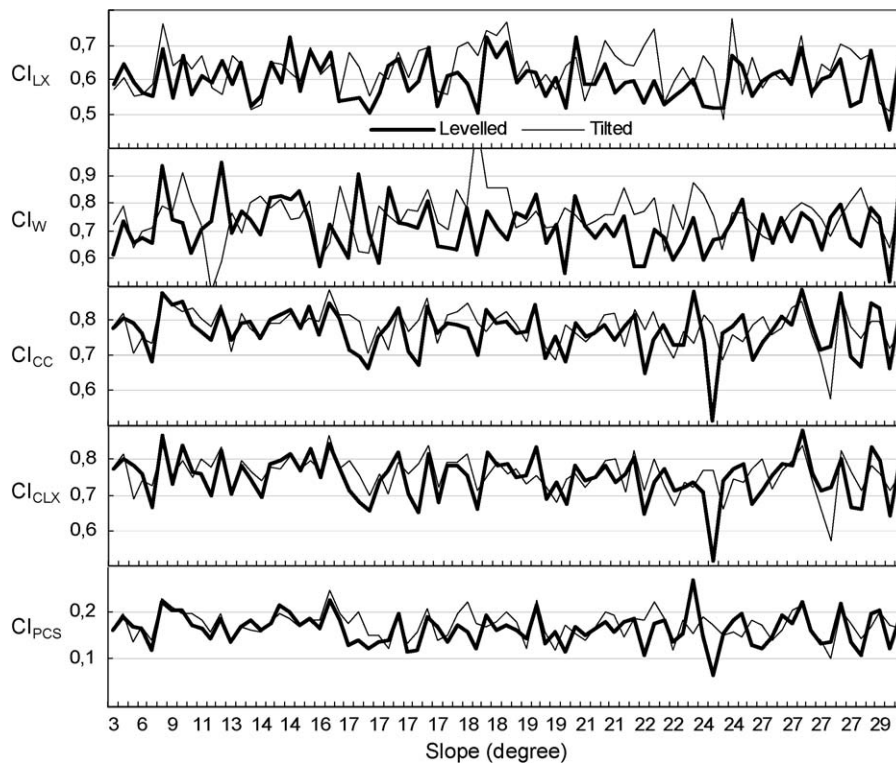


Fig. 4. Clumping index estimated using five methods for real photographs from levelled and tilted acquisition methods plotted against the slope gradient.

(Eq. (6)), whereas the second relies on a gap size distribution (Eq. (8)). 65% of CI_{LX} , 63% of CI_W , 57% of CI_{CC} , 57% of CI_{CLX} , and 60% of CI_{PCS} were resulted in lower CI from levelled acquisition compared to tilted acquisition. These indicate that the differences of estimates of CI from varying approaches regardless of slope or acquisition methods are not that of necessarily systematic.

Overall, acceptable correlations were obtained among the different CI approaches in both tilted and levelled acquisitions methods (Table 2). There is no clear difference of CI estimates along the severity of slope (Fig. 4). This is due to the fact that photo point based comparison shown in Fig. 4 is biased because of the view direction changes when the lens is tilted to the parallel of sloping ground. However, the overall comparison shows clear and consistent directions of differences among the CI calculation approaches and HP acquisition methods.

5. Conclusions

On HP taken normal to a horizontal surface (optical axis oriented to local zenith) on sloping ground, gap fractions and size distributions present strong upslope/downslope asymmetry of foliage elements. As the levelled acquisition is recommended for both canopy structure such as LAI, and solar radiation determination in forest ecosystem growing on complex topography (Gonsamo and Pellikka, 2008), it is indispensable to use the foliage clumping index approach which is less sensitive to the foliage density and the slope effect. Levelled HP resulted in lower CI (higher foliage clumping) compared to tilted acquisition. As demonstrated in both simulated and real HP analysis in this study, the combination of logarithmic gap averaging and gap size distribution approach, i.e., CI_{CLX} is preferred in all scenarios. The relationship between the real foliage element clumping and Pielou's coefficient of spatial segregation (CI_{PCS}) remains unexplained. However, the result obtained in this work warrants the further investigation of the use of CI_{PCS} for foliage element

clumping correction of LAI estimations. CI estimation from HP, other optical field instruments or remote sensing is fundamentally a complex 3D problem. Using a single 2D space such as gap fractions and size from HP, there is still a room for improvement of CI retrieval approaches either using the combination of methods shown in this study or using a fractal mathematics and dimension analysis to derive scale dependent heterogeneity indices.

Acknowledgments

We thank Jean-Michel Walter for CIMES programs package, simulated hemispherical photographs and valuable comments on the paper. This research was made possible by TAITA project: <http://www.helsinki.fi/science/taita/index.html> funded by Academy of Finland. The first author is financed partly by CIMO, Department of Geography of University of Helsinki, and the Finnish Graduate School of Geography.

References

- Chen, J.M., Liu, J., Leblanc, S.G., Lacaze, R., Roujean, J.-L., 2003. A demonstration of the utility of multi-angle remote sensing for estimating carbon absorption by vegetation. *Remote Sensing of Environment* 84, 516–525.
- Fournier, R.A., Landry, R., August, N.M., Fedosejevs, G., Gauthier, R.P., 1996. Modelling light obstruction in three conifer forests using hemispherical photography and fine tree architecture. *Agricultural and Forest Meteorology* 82, 47–72.
- Fournier, R.A., Rich, P.M., Landry, R., 1997. Hierarchical characterization of canopy architecture for boreal forest. *Journal of Geophysical Research* 102, 22445–22454.
- Gonsamo, A., Pellikka, P., 2008. Methodology comparison for slope correction in canopy biophysical parameters estimation using hemispherical photography. *Forest Ecology and Management* 256, 749–759.
- Gonsamo, A., Pellikka, P., Walter, J.-M.N., submitted for publication. Sampling gap fraction and size for estimating leaf area and clumping indices from hemispherical photographs. *Canadian Journal of Forest Research*.
- Jonckheere, I., Fleck, S., Nackaerts, K., Muysa, B., Coppin, P., Weiss, M., Baret, F., 2004. Review of methods for in situ leaf area index determination. Part I. Theories,

- sensors and hemispherical photography. *Agricultural and Forest Meteorology* 121, 19–35.
- Lang, A.R.G., Xiang, Y., 1986. Estimation of leaf area index from transmission of direct sunlight in discontinuous canopies. *Agricultural and Forest Meteorology* 37, 229–243.
- Leblanc, S.G., 2002. Correction to the plant canopy gap-size analysis theory used by the tracing radiation and architecture of canopies instrument. *Applied Optics* 31, 7667–7670.
- Leblanc, S.G., Chen, J.M., 2001. A practical scheme for correcting multiple scattering effects on optical LAI measurements. *Agricultural and Forest Meteorology* 110, 125–139.
- Leblanc, S.G., Chen, J.M., Fernandes, R., Deering, D.W., Conley, A., 2005. Methodology comparison for canopy structure parameters extraction from digital hemispherical photography in boreal forests. *Agricultural and Forest Meteorology* 129, 187–207.
- Macfarlane, C., Grigg, A., Evangelista, C., 2007. Estimating forest leaf area using cover and fullframe fisheye photography: thinking inside the circle. *Agricultural and Forest Meteorology* 146, 1–12.
- Miller, J.B., 1967. A formula for average foliage density. *Australian Journal of Botany* 15, 141–144.
- Pielou, E.C., 1962. Runs of one species with respect to another in transects through plant populations. *Biometrics* 18, 579–593.
- Walter, J.-M.N., Fournier, R.A., Soudani, K., Meyer, E., 2003. Integrating clumping effects in forest canopy structure: an assessment through hemispherical photographs. *Canadian Journal of Remote Sensing* 29, 388–410.
- Walter, J.-M.N., 2008. Hemispherical Photography of Forest Canopies. A Package of Programs for the Assessment of Canopy Geometry and Solar Radiation Regimes through Hemispherical Photographs. Université de Strasbourg, France. , <http://equinoxe.u-strasbg.fr/cimes>.